Significant Improvement in Bioavailability and Therapeutic Efficacy of Mebendazole Oral Nano-Systems Assessed in a Murine Model with Extreme Phenotypes of Susceptibility to Trichinella spiralis

Ana V. Codina , Paula Indelman , Lucila I. Hinrichsen , Maria Celina Lamas *

Posted Date: 27 April 2025

doi: 10.20944/preprints202504.2256.v1

Keywords: Mebendazole; Nano formulations; Animal model; Oral pharmacokinetics; Trichinellosis; Anthelmintic efficacy

 doi:10.20944/preprints202504.2256.v1

Article

Significant Improvement in Bioavailability and Therapeutic Efficacy of Mebendazole Oral Nano-Systems Assessed in a Murine Model with Extreme Phenotypes of Susceptibility to *Trichinella spiralis*

Ana V. Codina [a,b], Paula Indelman [c], Lucila I. Hinrichsen [a,b] and María C. Lamas [d,e,*]

[a] Instituto de Genética Experimental, Facultad de Ciencias Médicas, Universidad Nacional de Rosario, Santa Fe 3100, S2000KTR Rosario, Argentina
[b] CIC-UNR, Universidad Nacional de Rosario, Maipú 1065, S2000CGK Rosario, Argentina
[c] Área Parasitología, Facultad de Ciencias Bioquímicas y Farmacéuticas, Universidad Nacional de Rosario, Suipacha 531, S2002LRK Rosario, Argentina
[d] IQUIR-CONICET, Suipacha 570, S2002LRK Rosario, Argentina
[e] Departamento de Farmacia, Facultad de Ciencias Bioquímicas y Farmacéuticas, Universidad Nacional de Rosario, Suipacha 570, S2002LRK Rosario, Argentina
* Correspondence: authors:**Ana V. Codina**, Instituto de Genética Experimental, Facultad de Ciencias Médicas, Universidad Nacional de Rosario, Santa Fe 3100, S2000KTR Rosario, Argentina. **María Celina Lamas**, IQUIR-CONICET, Suipacha 570, S2002LRK Rosario, Argentina. Departamento de Farmacia, Facultad de Ciencias Bioquímicas y Farmacéuticas, Universidad Nacional de Rosario, Suipacha 570, S2002LRK Rosario, Argentina.
mail: mlamas@fbioyf.unr.edu.ar - lamas@iquir-conicet.gov.ar

Abstract: This study aimed to analyze whether enhancement of the biopharmaceutical efficiency of mebendazole (MBZ), a poorly water-soluble anthelmintic drug, significantly improves its antiparasitic activity in a murine model of trichinellosis. Two advanced oral formulations were developed: polyvinyl alcohol-derived nanoparticles (NP) and β-cyclodextrin citrate inclusion complexes (Comp). The NP and Comp formulations' physicochemical characteristics, pharmacokinetics, *in vitro* anthelmintic activity, and *in vivo* therapeutic efficacy against *Trichinella spiralis* encysted muscle larvae were examined. The formulations showed smaller particle sizes and enhanced dissolution properties than pure MBZ. The pharmacokinetics studies indicate that NP and Comp significantly improved MBZ bioavailability. The *in vivo* activity was assessed during the parenteral stage of *T. spiralis* infection in male and female mice from two genetically distinct lines differing in mebendazole pharmacokinetic parameters and susceptibility to the parasite. Both NP and Comp significantly increased mebendazole's anthelmintic activity against the encysted parasites, which would be attributed to the improved MBZ absorption provided by these innovative formulations. The formulations overcome the drug's poor solubility and low bioavailability limitations, resulting in a higher plasma concentration of the active drug, even at low doses. In summary, these findings suggest that **the newly designed** mebendazole formulations are suitable for treating ***T. spiralis* infection and** highlight a potential improvement in the **pharmacological treatment** of **trichinellosis**.

Keywords: Mebendazole; Nano formulations; Animal model; Oral pharmacokinetics; Trichinellosis; Anthelmintic efficacy

 doi:10.20944/preprints202504.2256.v1

1. Introduction

Neglected diseases are a diverse set of bacterial, viral, fungal, and parasitic infections considered endemic and affecting more than one billion people in 150 countries, mainly undeveloped or economically disadvantaged regions [1,2]. *Trichinella spiralis (T. spiralis)*, a nematode parasite that infests humans and a wide range of carnivorous and omnivorous mammals, is one such parasite that causes considerable morbidity and mortality. The parasite is metabolically and evolutionarily dependent on the host, creating a complex and permanent balance between both species [3] Though the host's immune response limits parasitic aggression, it usually does not achieve the elimination of the foreign agent [4]

Trichinellosis is the parasitic zoonosis caused by *Trichinella* spp., including *Trichinella spiralis*, which humans contract primarily through consuming undercooked or raw meat contaminated with encysted larvae [5]. It is a significant concern for public health, especially in regions with endemic outbreaks like Latin America [6,7]. It should be noted that trichinellosis is a reemerging disease and the seventh most important global parasitic infection [8,9]. The disease is characterized by its chronic nature, posing a significant challenge to healthcare systems worldwide. Diagnosis and treatment in the early stages are challenging, and effective procedures to limit the infection have not been found to date. The pharmaceutical therapy available for treating these parasitic diseases consists of several anthelmintic compounds, including mebendazole (MBZ) [10]. MBZ, a broad-spectrum anthelmintic compound used for treating and controlling several parasitic infections, is currently on the World Health Organization Model List of Essential Medicines. **It** is a member of the **benzimidazole family** of drugs and exhibits broad-spectrum anthelmintic activity. Its unique chemical structure and mechanism of action make it highly effective against various parasitic infections, including nematode infestations such as trichinellosis. While it is usually well-tolerated, it may present common side effects such as stomach pain, diarrhea, nausea, and dizziness. It is poorly water-soluble (1 μg/mL), and its oral bioavailability is approximately **20 %**, primarily due to its **poor absorption** and **extensive hepatic first-pass metabolism**. This low systemic availability significantly affects its **therapeutic efficacy** and overall clinical outcomes, particularly in systemic parasitic infections. The small amount of absorbed MBZ binds strongly to plasma proteins (95 %) and is rapidly and partially metabolized by the liver to form two predominant metabolites: methyl-5-(α-hydroxybenzyl)-2-benzimidazole carbamate and 2-amino-5-benzoylbenzimidazole.

In this context, designing and developing new pharmaceutical formulations is decisive in achieving optimal results after oral administration. We have been working on new derivatives of β-cyclodextrin (β-CD), a cyclic oligosaccharide composed of seven α-D-glucopyranose units linked by α-(1→4) glycosidic bonds. β-cyclodextrin is widely used in the pharmaceutical, food, and cosmetic industries due to its ability to form inclusion complexes with hydrophobic molecules, improving their solubility, stability, and bioavailability.

The new β-cyclodextrin derivative (citrate-β-cyclodextrin) exhibit enhanced water solubility, making an exceptional carrier for incorporating hydrophobic compounds [11].

Nanoparticles (NPs) are materials with dimensions in the nanometer (nm) range. Their small size endows them with unique physical, chemical, and biological properties, making them valuable in medicine, pharmaceuticals, and environmental applications. The increased surface area of nanoparticles enhances their solubility and absorption, further improving the bioavailability of active compounds. Nanoparticle based formulations using hydrophilic polymers, such as polyvinyl alcohol (PVA), serve as excellent delivery systems for active compounds administered by the oral route[12].

Therefore, the **primary goal** of this study was to develop **nanoparticles** and **inclusion complexes** of MBZ to enhance its **solubility**, **dissolution**, and **bioavailability**, thereby improving its therapeutic efficacy as an **anthelmintic** [13] The *in vivo* activity was evaluated during the parenteral stage of *T. spiralis* infection in males and females from two mouse lines differing in the novel formulations' pharmacokinetic parameters and susceptibility to the parasite. Using phenotypically defined animal models is a significant step forward in understanding the role of the host genetic background in resistance to parasitism and response to treatments. This approach may help identify

 doi:10.20944/preprints202504.2256.v1

the genes involved in the trait since genetic factors may influence a drug's efficacy and the likelihood of an adverse reaction. Comparative analysis of extreme response phenotypes, such as the ones used in these experiments, is instrumental in studies of the host-parasite relationship [14–17]and has been proposed as the procedure of choice in pharmacogenomics due to the phenotypes' "mendelian" nature [18]. Furthermore, it plays an important role in evaluating the efficacy and safety of new pharmaceutical devices as therapeutic alternatives for medical and veterinary use, potentially leading to more effective treatments.

2. Materials and methods

2.1. Materials

Mebendazole (MBZ) and β-cyclodextrin (β-CD) were supplied by Sigma-Aldrich Chemie GmbH (Steinheim, Germany). RPMI 1640 was obtained from Sigma-Aldrich Chemie GmbH (Steinheim, Germany), whereas fetal bovine serum and gentamicin were purchased from Klonal (Argentina). All other chemicals were of analytical grade.

2.2. Nanoparticle synthesis

MBZ (50 mg) was dissolved in formic acid (2.4 mL) and sonicated until complete dissolution. The resulting solution was dropped over an aqueous solution of polyvinyl alcohol (PVA, 10 mL, 0.5 % p/v) under magnetic stirring at 1000 rpm for 10 min. Then, the suspension was dried using a Mini Spray Dryer Buchi B-290 under the following controlled conditions: inlet temperature: 130 °C, outlet temperature: 60 °C, airflow: 30 m^3/h, feed rate 5 mL/min, and aspirator set 100 % [19]

2.3. β-cyclodextrin citrate and inclusion complexes synthesis

The β-cyclodextrin citrate (C-β-CD) and inclusion complexes were synthesized following the procedure outlined by García *et al.*(García et al. 2014) Briefly, citric acid (10.57 mmol, 2.03 g) was dissolved in water (1.2 mL), and β-CD (1.76 mmol, 2.00 g) was added in 1:6 molar ratio. The reaction mixture was refluxed at 100 °C for 6 h. Then, the product (C-β-CD) was precipitated employing isopropanol and centrifuged at 6000 rpm. The precipitate was washed twice with isopropanol to remove unreacted citric acid. Finally, C-β-CD was dried for 24 h at 60 °C, mortared, and stored in a tightly closed bottle until use. The inclusion complexes (Comp) were prepared using the spray drying method. MBZ (0.56 mol) was dissolved in formic acid (10 mL), and then C-β-CD (0.56 mol) and water (20 mL) were added to the solution. The resulting solution was dried in a Mini Spray Dryer Buchi B-290. The drying conditions were as follows: inlet temperature, 130 °C; outlet temperature, 70 °C; airflow, 38 m^3/h; pump efficiency, 12 % (flow rate ~5 mL/min); vacuum cleaner, 100 %.

2.4. Particle Size Determination

The particle size of the NP and inclusion complexes was determined by imaging using scanning electron microscopy (Leitz AMR 1600 T [Amray, Bedford, MA]), with an acceleration potential of 20 kV. Samples were sputter-coated with a gold layer to make them conductive. Then, to determine the particle size, scanning electron microscopy images were analyzed using the ImageJ software, a Java-based graphic design program dedicated to image analysis to estimate size. The particle size of nano-formulations was determined by using a Nano Particle Analyzer Horiba SZ-100 (Germany). Samples were diluted (1:30) in filtered distilled water before measuring.

2.5. Solubility and Dissolution Studies

The solubility of MBZ in the different formulations was determined by adding an excess amount in sealed vials with 5 mL of 0.1 N HCl in an orbital shaker at 180 rpm for 72 h. Afterward, the solutions were filtered through 0.45 mm PVDF filters, and the drug concentration was determined by UV spectroscopy at 285.0 nm (MBZ formulations) in a Shimadzu spectrophotometer. Dissolution studies of MBZ and MBZ formulations were performed using a Hanson Research SR8 8-Flask Bath

 doi:10.20944/preprints202504.2256.v1

equipment. The conditions were as follows: rotating paddle (apparatus II) speed of 75rpm (MBZ formulations), dissolution medium HCl 0.1 N (900 mL), and temperature of 37.0 ± 0.1 °C.

Dissolution efficiency of the dosage forms was calculated following the procedure proposed by Khan, 2015 [21]. For each formulation, the dissolution efficiency (DE) was calculated as the percentage ratio of the area under the dissolution curve up to time t to that of the area of the rectangle described by 100 % dissolution during the same time (Q100) using the following equation:

Dissolution efficiency:

$DE = (AUC \cdot t_0 / Q_{100} \cdot t) \cdot 100$

The area under the dissolution curve was calculated using GraphPadPrism 9.5 (GraphPadSoftware, San Diego, CA).

Solubility and dissolution experiments were carried out in triplicate. Following USP procedures [22]The dissolution medium for MBZ is 0.1 N HCl, which contains 1 % sodium lauryl sulfate, an anionic surfactant.

2.6. Animal model

Adult mice (80–90 days old) of lines CBi/L and CBi+ from the Animal Facilities of the Instituto de Genética Experimental, Facultad de Ciencias Médicas, Universidad Nacional de Rosario (CBi-IGE stock) were used. These lines, obtained by divergent selection for body conformation, are in the 160th generation of selective breeding, and their theoretical inbreeding coefficient is 0.99. The lines differ in body shape (CBi/L, low body weight-long-tail; CBi+, high body weight-long tail) and weight (mean ± SEM, g; CBi/L males 29.9 ± 0.23; CBi/L females 27.2 ± 0.21; CBi+ males 48.3 ± 0.48; CBi+ females 44.9 ± 0.55), and characters related to growth [23]. Previous experiments demonstrated that these lines also differ in response to infection with increasing doses of *T. spiralis* [24]. There was a significant difference in the infection intensity among genotypes. Though the larval muscle load increased as the infective dose rose, the magnitude of this increase was significantly different among lines: the analysis of variables that estimate the resistance/susceptibility of the host, such as intestinal parasite load and muscle larval load, allowed us to classify the CBi/L line as the resistant genotype and CBi+ as the most susceptible.

All the experiments with animals were done during the first half of the light cycle. Mice had access to complete balanced feed for rats and mice (Gepsa Feeds, Grupo Pilar S.A., Argentina) and water *ad libitum*. At the end of the experiment, mice were euthanized by inhalation of 70 % CO_2 using a chamber prepared *ad hoc* or by cervical dislocation.

Mice were handled according to the institutional regulations (Facultad de Ciencias Médicas, Universidad Nacional de Rosario, permit number 1926/2020), which comply with the guidelines issued by the Institute for Laboratory Animal Resources, National Research Council (2011).

2.7. Parasite

T. spiralis was generously provided by Dr. Maria Dalla Fontana (Laboratorio de Zoonosis, Laboratorio Central de la Red Provincial de Laboratorios, Dirección de Bioquímica y Farmacia, Santa Fe, Argentina). This parasite has been maintained in CBi mice since 2006. The strain was genotyped as *T. spiralis* using multiplex polymerase chain reaction (Dr. Silvio Krivokapich, Departamento de Parasitología, Administración Nacional de Laboratorios e Institutos de Salud 'Dr. Carlos Malbrán', Buenos Aires, Argentina, personal communication).

The L1-infective larvae used in the infection were recovered by artificial digestion from the muscles of mice from line CBi, infected 3–4 months earlier for that purpose, as described previously [24]

2.8. In vitro analysis of the anthelmintic activity of the MBZ formulations

2.5.1. Preparation of T. spiralis female worms

CBi mice given an oral dose of 10 L1 *T. spiralis* larvae per g body weight were sacrificed in the intestinal phase of the infection on day 6 post-infection (p-i), as already described [24]. The animals

 doi:10.20944/preprints202504.2256.v1

were euthanized, the small intestine was removed, cut into several pieces of roughly equal length, and placed on Petri dishes with 8-12 mL of 0.85 % NaCl plus 250 µg/mL gentamicin (incubation medium). Each piece was then opened lengthwise using small iris scissors, grasped with forceps, agitated gently in the medium, and incubated for 4 h at 37 °C in 5 % CO_2. After incubation, the pieces of the intestine were rinsed with the medium onto the Petri dish and discarded. All the content of the Petri dishes was transferred to centrifuge tubes and centrifuged at low speed. The parasite pellet was resuspended in approximately 2-3 mL RPMI 1640 medium supplemented with gentamicin and fetal bovine serum (250 µg/mL and 10 % v/v, respectively) and placed in a sterile plate to identify and separate the female worms for the assay.

2.8.2. Preparation of the antiparasitic solutions

As described elsewhere [11] MBZ, NP, and Comp stock solutions were prepared at a 10 mg MBZ/mL concentration in dimethyl sulfoxide (DMSO). Briefly, the working solutions were formulated with RPMI 1640 medium containing gentamicin (250 µg/mL) and DMSO (up to a maximum of 2 %) to obtain a final concentration of 500 µg/mL of MBZ. They were stirred at room temperature for 24 h and then filtered through sterile ethyl cellulose filters 0.2 µm pore (Minisart®, Sartorius Stedim Biotech, USA).

2.8.3. In vitro assay

The entire procedure was done under sterile conditions, as Priotti *et al*. [12] described. *T. spiralis* female worms obtained as explained above were incubated overnight in RPMI 1640 supplemented with gentamicin (250 µg/mL) and fetal bovine serum (10 % v/v) at 37 °C in a 5 % CO_2 atmosphere before being used. For the assay, females were placed in 24-well cell culture plates (10 to 12 per well) containing the antiparasitic MBZ formulations to be tested supplemented with 10 % fetal bovine serum. The MBZ solution was used as a positive control, and the culture medium with the solvent was employed as a negative control. The worms were incubated in a humid 5 % CO_2 atmosphere at 37 °C for 30 h and were observed with an inverted microscope at 2, 4, 7, 24, and 30 h. Female viability was estimated at each time point by analyzing its motility and morphology to count it as "live" or "dead." The amount and motility of newborn larvae were also examined. The effect of the various antiparasitic solutions on median worm survival was estimated using a survival curve analysis.

Each experiment was performed in duplicate, and data were corrected with the negative control.

2.9. Pharmacokinetic analysis

The preparation and administration of the solid dosage forms were performed following the protocol outlined by Codina *et al* [25]. A pure or formulated MBZ suspension was mixed with glycerin (50 mg powder/1 g glycerin) and sonicated to homogenize. Aliquots of this suspension were added to Eppendorf® tubes to reach the dose of 15 mg MBZ/kg mean body weight for each line and sex. Separately, 2.6 g gelatin powder was solubilized in 10 mL hot water (60 °C) to obtain a solution; before the gelatin solidified, an aliquot of this solution (100 µL) was added to the Eppendorf® tube containing the glycerin suspension. Next, the mixture was sonicated in a water bath at 60 °C, and 40 mg of powdered commercial chow was incorporated to make the preparation palatable so that mice would eat it without waste. The final pharmaceutical dosage form contained pure MBZ or the formulation, gelatin, and food powder. Glycerin and gelatin are GRAS (Generally Recognized as Safe) excipients listed as inactive ingredients by the U.S. Food and Drug Administration. Finally, the formulations were stored at 4 °C until administration.

CBi/L and CBi+ males and females were fasted for approximately 12 h, with free access to water (n = 93–99 per line and sex), and randomly divided into three groups to receive a single oral dose of pure MBZ, NP, or Comp prepared as described. Following the procedures described by Codina *et al*. [26], three to four animals per formulation were anesthetized after the drug administration with an intraperitoneal injection of ketamine/xylazine 10:1, 5 min before blood collection. Whole blood (approximately 1.5 mL) samples were taken by cardiac puncture at 0.3, 0.6, 1, 1.2, 2, 2.5, 3, 4, 5, 7, and

 doi:10.20944/preprints202504.2256.v1

24 h post-treatment. Blood was collected into heparinized vials and centrifuged at 9000 rpm for 15 minutes to obtain plasma, which was transferred to a plastic tube and stored at -20 °C until HPLC analysis.

2.9.1. HPLC analysis

The MBZ plasma concentration of each mouse was quantified by HPLC analysis using a UVDAD detector (Agilent 1260 HPLC DAD). Briefly, each plasma sample (200 µL) was treated to eliminate proteins by adding methanol (1 mL), frozen for 30 min at -20 °C, and centrifuged at 15000 rpm at 4 °C for 12 min. Then, the supernatant was evaporated under vacuum, and the dried samples were frozen until analyzed. Samples were resuspended in 100 µL of mobile phase and filtered through 0.2 µm polyvinyl difluoride syringe filters (Agilent). The mobile phase consisted of 0.05 M monobasic potassium phosphate buffer/methanol (40:60, v/v). Samples of 25 µL were injected, and the analytes were eluted (flow 1.2 mL/min) from a column Zorbax Eclipse C-18 (150 × 4.6 mm; 5 µm). The absorbance was measured at a wavelength of 247 nm. The analyte retention time was 3.8 ± 0.2 min. A calibration curve was made with a control concentration MBZ, range of 0.25-4 µg/mL (R^2 = 0.99). MBZ was determined by comparing retention times with those of a pure reference standard[27].

2.9.2. Pharmacokinetic parameters

To estimate MBZ bioavailability in the different formulations, the parameters maximum plasma concentration (C_{max}), time to achieve the maximum plasma concentration (T_{max}), and areas under the concentration-time curve from 0 to 7 h (AUC_{0-7}) and from 0 to 24 h (AUC_{0-24}) were measured[28]. AUCs were calculated using the trapezoidal rule. Pharmacokinetic parameters were expressed as mean ± SEM. The NP and Comp systems' relative bioavailability (AUCr, %) was calculated for each group as follows:

$$AUC_r = AUC_{system} / AUC_{MBZ} .100$$

where AUC_{MBZ} is the mean value of the corresponding genotype and sex.

2.10. In vivo analysis of the anthelmintic activity of pure MBZ and its formulations

2.10.1. Infection

Since CBi/L and CBi+ mice show significant body weight differences, as already stated, adult animals of both sexes were infected orally with an equivalent dose of 2 *T. spiralis* L1 larvae per gram of the host's body weight. Each animal was weighed before infection, 24–48 hours before treatment, and before sacrifice. During the infection course, the general health of each mouse (overall physical condition and behavior) was monitored three times a week [29].

2.10.2. Assessment of the new formulations' therapeutic efficacy

The anthelmintic activity of pure MBZ and its new formulations were evaluated in the parenteral stage of the parasite cycle. A single daily oral dose of MBZ, NP, or Comp was given to each mouse (15 mg MBZ/kg body weight/day) in the parenteral phase of the infection on days 27, 28, and 29 p-i. Six mice per line and sex were randomly assigned to the non-treated control (C) or treated groups (MBZ, NP, or Comp). Seven days after the last dose, mice were sacrificed to determine the number of encysted muscle larvae in the tongue. Briefly, the tongue was excised, weighed, and subjected to artificial pepsin–HCl digestion, and after overnight incubation at 37 °C, the digestion was stopped by adding saline. Next, the larvae were rinsed with saline several times to remove debris, and the supernatant was gently removed after centrifugation at a very low speed (250 – 300 g) for 5 min. Finally, the pellet containing all the tongue's encysted larvae was resuspended in 2 mL saline and placed in an acrylic plate to count them under an optical microscope at 40× magnification.

Each formulation's anthelmintic efficacy was assessed by its effect on the larval muscle load (relative larval load: rLL, number of L1 larvae per g fresh tissue). Also, the effect of the formulations on the encysted L1 larvae viability (dead larvae percentage: proportion of dead muscle larvae/total

 doi:10.20944/preprints202504.2256.v1

muscle larvae recovered from each animal) was analyzed using the methylene blue supravital staining technique, as already described [30].

2.10.3. Assessment of increasing doses of pure MBZ on its therapeutic efficacy

Higher concentrations of pure MBZ were administered to determine whether increasing the dose significantly improved the drug's therapeutic outcome. Briefly, adult susceptible CBi+ mice of both sexes orally infected with 2 *T. spiralis* L1 larvae/g of the host's body weight were randomly assigned (n = 4 per sex, per treatment) to non-treated control (C) or treated groups receiving a daily dose of 30 or 45 mg MBZ/kg body weight. As in the experiments described in section *2.10.2*, the pure drug was administered in the parenteral stage of infection on days 27, 28, and 29 post-infection. Seven days after the last dose, mice were sacrificed, and the number and viability of the tongue's encysted muscle larvae were determined to evaluate anthelmintic efficacy. The results were compared with those obtained from animals treated with the pure drug or the formulations at a dose of 15 mg MBZ/kg body weight.

2.11. Statistical analysis

Survival curves were calculated using Kaplan and Meier's product limit method (GraphPad Prism® 9.5; GraphPad Software, Inc., San Diego, California, USA). The significance of the difference among survival curves was determined with the log-rank test.

The statistical significance of the differences among treatment groups was assessed with a one-way analysis of variance (ANOVA), followed by Tukey post-test or the nonparametric Kruskal-Wallis' test and Dunn's test, as appropriate [31]. Comparisons between sexes within genotype and treatment were analyzed with Student's t-test or the nonparametric Mann-Whitney test. Differences were considered significant if $P < 0.05$.

3. Results and discussion

3.1. Particle Size, Solubility, and Dissolution Studies

The physicochemical characteristics of the new formulations were studied, and particle size, solubility, dissolution efficiency (DE), and dissolution rate (DR) were measured (Table 1).

Table 1. Solubility and dissolution efficiency and particle size of the different formulations.

Drug	Solubility in HCl 0.1 N (mg/ml)	Solubility increase (fold)	Dissolution Efficiency (%)	Dissolution Efficiency Increase (fold)	Particle size#
MBZ	0.025 ± 0.003	-	20.6 ± 0.1	-	---
MBZ-NP	0.53 ± 0.040	21	74.2 ± 0.5	7	500 nm
MBZ-Comp	2.015 ± 0.009	81	87.4 ± 0.3	8	5 µm

mean diameter.

The novel systems, nanoparticles (NP) and β-cyclodextrin inclusion complexes (Comp) showed decreased particle size and improved solubility and DR compared with the pure drug. In both formulations, MBZ particles' size decreased by 2-98 times: Comp exhibited particles with less than 5 µm mean diameter, and NP nanoparticles were under 500 nm and monodispersed.

NP increased MBZ solubility and DR but to a much lower extent than the pure drug. Comp presented the best dissolution profile, indicating that β-cyclodextrin citrate should be the excipient of choice to improve the solubility of poorly water-soluble active pharmaceutical ingredients. It should be expected that, as particle size decreases, the aqueous solubility properties of the new orally

 doi:10.20944/preprints202504.2256.v1

bioavailable MBZ formulations improve positively, thereby impacting the drug's systemic absorption [32].

3.2. In vitro assay

Figure 1 and Table 2 show the effect of NP and Comp on the survival curves and survival parameters of the female parasites cultured for 30 h in medium RPMI 1640 containing the MBZ formulations. The Kaplan-Meier estimates revealed a lower survival time for the new MBZ systems, thus improving MBZ parasiticidal activity (P = 0.023). The NP formulation was considerably more efficient than pure MBZ (P = 0.009), with a median survival of 30 h and a proportion of live worms of 47.6 % at the end of the experiment; the survival estimates of Comp did not differ significantly from that of the pure drug in the period analyzed.

The effect of the formulations on the newborn larvae released by *T. spiralis* females exposed to the antiparasitic solutions was also examined. Neither MBZ nor the formulations affected the mobility of the *T. spiralis* newborn larvae during the studied period, notwithstanding that fewer larvae were observed in the wells containing the NP system.

It is known that increasing the solubility of an active pharmaceutical ingredient can be achieved by "particle size reduction," which leads to an increase in surface area and a faster dissolution rate [33–36]. The particle size of the nanoparticles in this formulation was small enough to facilitate the rapid passage of the drug through the cuticle of *T. spiralis* females, thus disrupting the reproductive capacity of the female worms and producing some degree of infertility during the *in vitro* assay.

The NP formulation's significant improvement in efficacy suggests that it could be a promising alternative to traditional MBZ treatments.

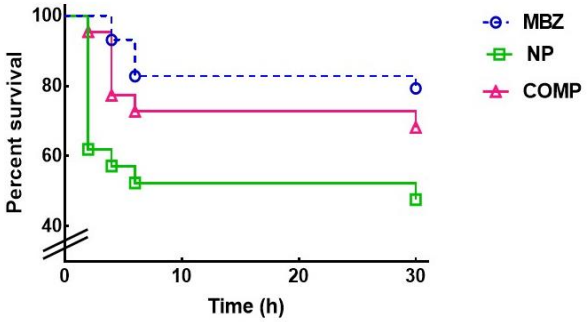

Figure 1. Analysis of the *in vitro* parasiticidal effect of the MBZ pure drug and the new formulations on *T. spiralis* adult worms. Survival curves of *T. spiralis* females cultured with the different MBZ antiparasitic solutions were generated using the Kaplan-Meier product limit method. The significance of the differences between curves was estimated with the log-rank test.

Table 2. Effect of the MBZ formulations on the survival parameters of *T. spiralis* females after 30 h incubation in RPMI 1640 medium containing the MBZ systems.

Formulations	Median survival (hours)	Survival proportion after 30 h (%)
MBZ [a]	Undefined	79.3
NP [b]	30	47.6
Comp [a]	Undefined	68.2

Data in the table are derived from the Kaplan-Meier survival curves generated with GraphPad Prism version 9.5. The significance of the differences among formulations was calculated with the log-rank test. Groups not sharing the same superscript differ significantly (P < 0.025).

Preprints.org (www.preprints.org) | NOT PEER-REVIEWED | Posted: 27 April 2025 doi:10.20944/preprints202504.2256.v1

3.3. Pharmacokinetic analysis

The NP and Comp systems' bioavailability was evaluated by measuring MBZ plasma concentration levels and comparing them to pure MBZ. Figure 2 shows the plasma levels of MBZ as a function of time after a single oral dose of pure MBZ, NP, or Comp given to CBi/L and CBi+ animals of both sexes. Tables 3 and 4 summarize the pharmacokinetic parameters maximum plasma concentration (C_{max}), time to reach the maximum concentration (T_{max}), and area under the plasma drug concentration *versus* time curve (AUC), derived from the bioavailability curves for CBi/L and CBi+ mice, respectively.

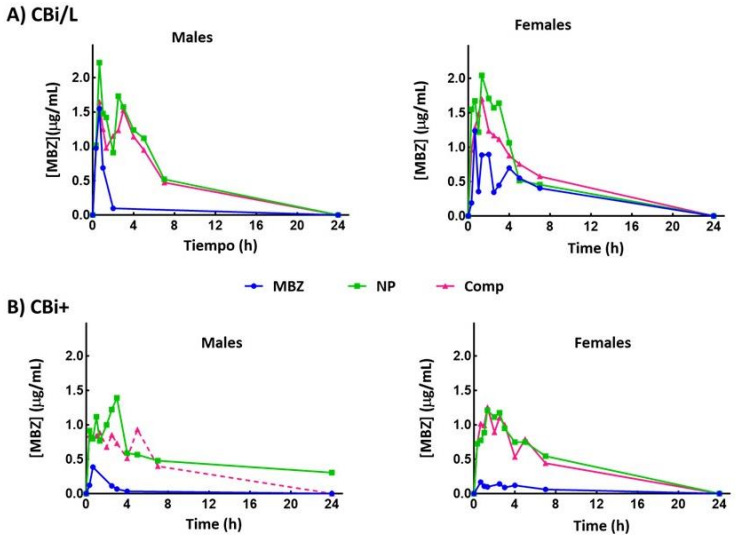

Figure 2. Plasma MBZ concentration-time profiles after oral administration of a single dose of pure MBZ, NP, or Comp (dose, 15 mg MBZ/kg body weight) to male and female mice of the lines CBi/L (A) and CBi+ (B). Each time point represents the mean ± SEM of 3 mice.

Two of the three bioavailability parameters examined in this analysis, C_{max} and AUC, showed a genotype effect in the MBZ group: CBi/L mice had significantly higher C_{max} (♂ P = 0.044; ♀ P = 0.007) and AUC (♂ P = 0.085; ♀ P = 0.014) values than CBi+ animals. The variation in the pharmacokinetic response observed in this group is only attributable to the host's genotype [37,38] since the parameters did not show a sex effect**.**

Formulating drugs with poor water solubility as nanoparticles or **cyclodextrin complexes** has proven to be an effective strategy for increasing the drug's **plasma levels.**

Table 3. Pharmacokinetic parameters for MBZ obtained after oral administration of MBZ, NP, or Comp to male and female CBi/L mice*.

Parameter	Sex	Formulations		
		MBZ	NP	Comp
C_{max} (µg/mL) #	♂	1.3 ± 0.31 [a]	2.3 ± 0.28 [b]	1.7 ± 0.42 [a, b]
	♀	1.3± 0.26 [a]	2.2 ± 0.08 [b]	1.7 ± 0.20 [a, b]
T_{max} (h)	♂	0.66	0.66	0.66
	♀	0.66	1.33	1.33
$AUC_{0-7\ h}$ (µg.h/mL) #	♂	2.7 ± 0.82 [a]	8.2 ± 0.34 [b]	5.1 ± 1.00 [a, b]
	♀	3.9 ± 0.63 [a]	7.4 ± 1.16 [a]	6.4 ± 1.24 [a]

 doi:10.20944/preprints202504.2256.v1

$AUC_{0\text{-}24\ h}$ (μg.h/mL) #	♂	8.4 ± 3.37 [a]	12.6 ± 0.69 [a]	14.1 ±2.30 [a]
	♀	7.2 ± 1.53 [a]	11.3 ± 2.29 [a]	11.1 ± 1.10 [a]
$AUCr_{0\text{-}7\ h}$ (%)	♂	---	204	88
	♀	---	90	64
$AUCr_{0\text{-}24\ h}$ (%)	♂	---	50	67
	♀	---	57	54

*Mice were given a single oral dose of 15 mg MBZ/kg body weight. MBZ: pure mebendazole; NP: MBZ nanoparticles; Comp: MBZ inclusion complex with β-cyclodextrin citrate. # Mean ± SEM. Differences among the treatment groups within sex were estimated using a parametric ANOVA followed by Tukey´s multiple comparisons test. In each row, groups that do not share the same superscript are significantly different (P <0.025).

Table 4. Pharmacokinetic parameters for MBZ obtained after oral administration of MBZ, NP, or Comp to male and female CBi+ mice*.

Parameter	Sex	Formulations		
		MBZ	NP	Comp
C_{max} (μg/mL) #	♂	0.3 ± 0.11 [a]	1.5 ± 0.08 [b]	1.1 ± 0.04 [c]
	♀	0.2± 0.02 [a]	1.3 ± 0.09 [b]	1.4 ± 0.08 [b]
T_{max} (h)	♂	0.66	3	5
	♀	0.66	1.33	1.33
$AUC_{0\text{-}7\ h}$ (μg.h/mL) #	♂	0.4 ± 0.20 [a]	5.4 ± 0.18 [b]	4.7 ± 0.50 [b]
	♀	0.6 ± 0.08 [a]	5.7 ± 0.35 [b]	5.3 ± 0.63 [b]
$AUC_{0\text{-}24\ h}$ (μg.h/mL) #	♂	0.7 ± 0.33 [a]	9.8 ± 2.54 [b]	8.1 ± 1.13 [b]
	♀	1.8 ± 0.40 [a]	10.1 ± 0.62 [b]	9.0 ± 1.98 [b]
$AUCr_{0\text{-}7\ h}$ (%)	♂	---	1250	1175
	♀	---	850	783
$AUCr_{0\text{-}24\ h}$ (%)	♂	---	1300	1057
	♀	---	461	400

*Mice were given a single oral dose of 15 mg MBZ/kg body weight. MBZ: pure mebendazole; NP: MBZ nanoparticles; Comp: MBZ inclusion complex with β-cyclodextrin citrate. # Mean ± SEM. Differences among the treatment groups within sex were estimated using a parametric ANOVA followed by Tukey´s multiple comparisons test. In each row, groups that do not share the same superscript are significantly different (P <0.025).

This enhancement directly addresses the limitations of poor bioavailability, allowing for improved systemic drug exposure and therapeutic outcomes [39,40]. In this animal model, the effect of NP or Comp on MBZ bioavailability depends on both the host genotype and sex. In CBi/L mice (Table 3), NP led to a higher plasma concentration and a significantly increased C_{max} compared to animals receiving pure MBZ (♂ P = 0.04; ♀ P = 0.01); mice given Comp showed a nonsignificant increase in the parameter (P > 0.05). Conversely, in CBi+ mice (Table 4), both NP and Comp led to a higher C_{max} than those treated with pure MBZ (♂ P = 0.0002; ♀ P < 0.0001). Notably, only CBi+ males showed differences between formulations: NP improved C_{max} compared with those receiving

 doi:10.20944/preprints202504.2256.v1

Comp (♂ P = 0.0029). This difference between formulations was not observed in CBi+ females nor CBi/L animals (P > 0.5), thus implying a genotype x sex interaction in the MBZ formulations' bioavailability [41]. T_{max} values also showed genotype and sex effects in the groups receiving the formulations. Regardless of genotype, females given NP or Comp doubled the T_{max} value obtained in the MBZ group; CBi/L males administered the new systems did not modify T_{max}, while CBi+ males increased it 3 to 4-fold (Table 4). These results also reveal a genotype x sex interaction for Tmax. In summary, the rate of absorption of MBZ estimated by both T_{max} (an indirect and approximate measure of the duration of the absorption process) and C_{max} (partly determined by the balance between rates, rate of entry, and rate of exit) was affected by the sex and genotype of the host in this animal model.

Differences attributable to genotype were also observed in bioavailability after oral administration, estimated by computing AUC. AUC increased in all CBi/L groups (Table 3), as reflected in AUCr; however, only CBi/L males given NP had a significantly higher AUC_{0-7} than those receiving pure MBZ (P = 0.004). CBi+ males and females treated with NP or Comp (Table 4) significantly increased AUC_{0-7} compared to pure MBZ (♂ P = 0.015; ♀ P = 0.006), but there were no significant differences between the formulations (P > 0.05). Although AUC_{0-7} and AUC_{0-24} did not show a significant sex effect (P > 0.05) in any formulation, in both genotypes, the relative bioavailability (AUCr) showed differences between sexes. Males given NP or Comp had an average higher increase in $AUCr_{0-7}$ than females of the same genotype and treatment group. CBi+ males displayed higher values than CBi+ females in $AUCr_{0-24}$ for both formulations.

Biological sex is a significant source of variation in the responses to pharmacological treatments due to its effect on genes involved in the metabolism and transport of the active pharmaceutical ingredient and excipients [42] the magnitude of sex differences depends on the substrates and metabolic pathways involved [43]. Additionally, recent reviews have emphasized the role of sex as a biological variable significantly influencing the efficacy and toxicity of therapeutic nanomaterials. There is compelling recent evidence that sex differences can alter the efficacy of nanoparticles at the cellular level. Among other factors, the level and pathway of nanoparticle uptake and intracellular trafficking in certain human cells are heavily influenced by sex; furthermore, the composition of the biomolecular/protein is affected by sex-specific paracrine factors [44] Anatomical and physiological differences between sexes impact nano drugs' four main processes: absorption, distribution, metabolism, and excretion [45]. There are some differences in the functioning of the gastrointestinal system between males and females. Female sex hormones, gastric hormone receptors, and nitric oxide influence gastric motility, likely resulting in decreased contraction frequency and slower gastric emptying, as observed in rats. Sex-dependent differences in body composition can also affect the distribution of pharmacological or non-medicinal formulations: males and females have distinct total body water distribution and differences in muscle and fat distribution.

The observed differences could also involve cytochrome P450 enzymes. *CYP* genes are highly polymorphic and represent a significant pharmacokinetics and drug response variability source. Additionally, several *CYP* genes have been documented to have sex-dependent expression or activity in rodents and humans [46–48]. CYP3A4 is a critical hepatic cytochrome that metabolizes up to 50 % of all drugs and is the most abundant CYP isoenzyme in the human liver. Most clinical studies indicate that women metabolize drugs faster than men [49], as was observed in our animal model; though not significant, females tended to achieve a lower AUC than males. Recognizing the sources and understanding the factors contributing to pharmacokinetic and pharmacodynamic variability within and between individuals remains a significant challenge, especially for drugs with a narrow therapeutic index [50,51].

3.4. In vivo anthelmintic activity of MBZ formulations

The ***in vivo*** **therapeutic efficacy** of the **MBZ** formulations and the comparison of their effectiveness with that of the **pure drug were** assessed in the **chronic stage of the infection** with *Trichinella spiralis in mouse lines CBi/L and CBi+ of the CBi-IGE animal model of trichinellosis (Table 5) [24].*

 doi:10.20944/preprints202504.2256.v1

During this study, animals neither significantly changed their body weight nor showed signs of impaired health status. Also, signs or symptoms of trichinellosis or adverse effects resulting from the treatments were not observed.

The level of infection in each animal, measured through the relative muscle parasite burden (rLL), showed significant differences between lines.

As expected, CBi/L mice of the control group showed significantly lower rLL than CBi+ controls ($P < 0.001$). This result is directly related to genotypic differences between these lines: CBi/L behaves as resistant against infection with *T. spiralis* and has a very low parasite load compared to the highly susceptible CBi+ genotype. Contrary to what other authors have observed, treatment with pure MBZ on days 27, 28, and 29 post-infection did not reduce the number of muscle larvae recovered compared to the control animals. The different responses could result from using dissimilar treatment protocols, mainly higher doses of MBZ, either administered twice a day or for more extended periods [52–54].

As stated by Wesołowska [55], the sex of a host affects the intensity, prevalence, and severity of helminth infection. One sex may be more susceptible than the other, with the prevalence and intensity of helminth infections being generally higher among male than female hosts. Nevertheless, exceptions may exist. Table 4 shows that rLL on day 37 p-i was significantly lower in animals treated with NP or Comp compared to control or pure MBZ groups, regardless of genotype and sex. However, CBi/L females and males did not respond equally to treatment; females showed a higher muscle larval load than males in the three treatment groups ($P < 0.05$). This sex effect was not observed in treated CBi+ mice or the control groups.

The improvement in therapeutic efficacy achieved with the MBZ formulations was also observed when determining the viability of the recovered muscle larvae. Though CBi/L and CBi+ control animals showed significant differences in the proportion of dead L1 larvae, the treatment groups did not exhibit this genotype effect. Males and females from both lines, given NP or Comp, showed a major increase in the proportion of dead larvae, as estimated using the methylene blue test. CBi+ males and females and CBi/L females receiving the formulations showed a significantly higher proportion of dead larvae compared to their controls or MBZ-treated groups (CBi+: ♂ $P = 0.0043$; ♀ $P = 0.0005$; CBi/L: ♀ $P = 0.0122$). Though CBi/L males given the formulations also showed an increase in the proportion of dead larvae, the difference was not statistically significant. The lack of significance would be, in part, a consequence of a reduction in the sample size since of the six male mice studied in each group, L1 larvae were not recovered in 3 animals of the NP group and 1 of the Comp group.

CBi+ males and females treated with 30 or 45 mg MBZ /kg showed a 40 % decrease in muscle rLL compared with the control mice or treated with 15 mg MBZ/kg (Figure 3).

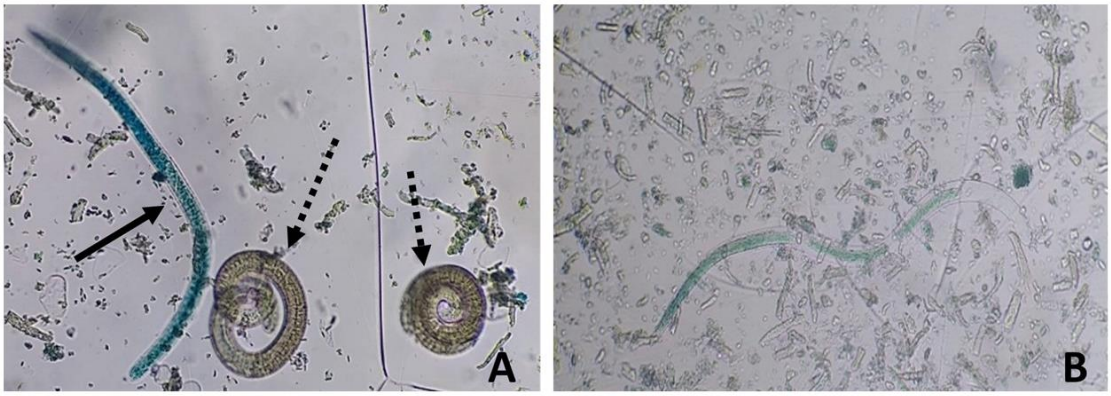

Figure 3. Representative micrographs of *Trichinella spiralis* L1 larvae recovered after artificial digestion of the tongue of mice in the chronic stage of the infection, stained with the methylene blue supravital technique (magnification 40X). A) The solid arrow indicates a dead L1 larva obtained from a mouse treated with MBZ showing the characteristic "comma" shape and blue color; dashed arrows point to live, unstained L1 larvae. B)

 doi:10.20944/preprints202504.2256.v1

Dead, non-viable L1 larva from an NP-treated mouse exhibiting an altered internal morphology and light blue staining (solid arrow).

However, despite increasing the dose of pure MBZ, animals treated with NP or Comp still showed a significantly lower muscle load (♂, $P < 0.0001$; ♀, $P = 0.0036$) and a higher dead larvae percentage compared with the pure MBZ (♂, $P = 0.0005$; ♀, $P < 0.0001$). The efficacy of increased MBZ dosage in treating *T. spiralis* infection was low compared to what other investigators have reported. This variation in the response observed among experiments could be due to different treatment regimens, parasite strains, and experimental models.

Figure 4 shows dead larvae recovered from mice of either sex or genotype treated with NP or Comp, which exhibited a highly altered internal structure. Furthermore, they were [56–59] stained in a light blue, [60]almost transparent color and localized on the solution's surface (Fig. 4B). In contrast, dead larvae obtained from MBZ-treated animals showed a dark blue stain, maintained the typical internal structure, and were found at the bottom of the plate (Fig. 4A).

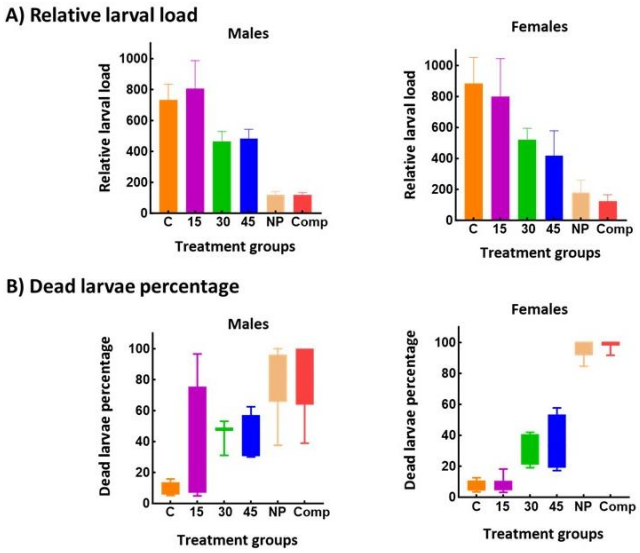

Figure 4. Comparative study of the therapeutic efficacy of increasing mebendazole dose *vs*. a low dose of the new formulations in *T. spiralis*-infected CBi+ mice. The drug was administered in the chronic stage of the infection. A) **Relative larval load**: total muscle-encysted larvae per g of fresh tissue. Larval load was measured in the tongue, a preferred site of encystment in mice. B) **Dead larvae percentage**: proportion of dead muscle larvae/total muscle larvae recovered from each animal. The significance of the differences among groups was evaluated by a one-way ANOVA, using Bonferroni's post-test for comparisons between groups (Relative larval load) or by the nonparametric Kruskall-Wallis' test and Dunn's test for between-groups comparison (Dead larvae percentage).

During the parenteral phase, *T. spiralis* larvae penetrate muscle cells, modifying them and creating a protective niche known as a nurse cell or larval cyst, a new capillary network, originating from pre-existing blood vessels and required for the larvae's nutrition and waste elimination, forms on the surface of the nurse cell. The larva/nurse cell complex is characterized by promoting chronic inflammation at the site of infection, sustained by the "invasion" of the infected muscle tissue by the host's immune cells that attempt to destroy it [61]. Histological studies by other authors concluded that MBZ acts primarily on the tissue surrounding the larvae, causing larval metabolites and antigens to enter the host's circulation, eliciting more intense immune and inflammatory responses. MBZ induces significant degenerative changes in the nurse cells, allowing inflammatory cells to infiltrate and ultimately destroy the parasite. The anthelmintic action of MBZ disrupts the cellular components of the cell matrix, turning each larva into an exposed antigenic focus that triggers cell-mediated immunity. Notably, 80 to 100 % of the larvae recovered from CBi/L and CBi+ males and females

 doi:10.20944/preprints202504.2256.v1

treated with NP and Comp formulations were dead and showed destroyed internal structures. In contrast, the few dead larvae recovered from animals treated with MBZ retained their internal conformation. If the anthelmintic action of MBZ in the muscle phase is the result of combined pharmacological and immunological effects, it could be hypothesized that a larger number of dead larvae would stimulate a stronger immune response, leading to the destruction of the parasite's internal structure, potentially resulting in the total disintegration of the larva. Such a situation could explain the results obtained in male CBi/L mice, in which no muscle larvae were recovered, and the finding of the differences in the structure of the dead larvae from each treatment group.

While MBZ has demonstrated a considerable effect on all stages of the *T. spiralis* life cycle in mice treated with high doses, its use would be limited in clinical practice since MBZ has been found effective only against newborn larvae present in blood vessels and lymphatics, but not against larvae encapsulated in muscle cells [62]. Treatment of human trichinellosis is a complex matter since antiparasitic treatment, control of inflammation, analgesic and symptomatic medication, and rehabilitation in the case of chronic trichinellosis should be considered [63]. Prolonged oral high-dose MBZ therapy may provide an effective anthelmintic response, but side effects such as Herxheimer-like reactions may occur after the initiation of the specific treatment. These reactions are usually observed following the massive discharge of antigenic molecules and immunologic stimulation and can also be noticed in heavy infections. It should be stressed that MBZ is not recommended for treating human trichinellosis in the muscle phase, as exacerbating the immune response generated by the presence of the encysted larvae could provoke, as noted above, a reaction similar to a dangerous anaphylactic shock [64].

4. Conclusions

The results showed that both formulations improved the therapeutic efficacy of MBZ in genetically different hosts, reducing the parasitic load by 80-90 %. In the animal model employed, the host's genotype contributed noticeably to the expression of sex differences in its pharmacokinetic and therapeutic responses. The **bioavailability analysis** of **pure** MBZ revealed that **host genotype** and **sex** significantly influenced the pharmacokinetic parameters of the drug. While these effects were observed to a lesser degree in animals administered the formulations, they still played a role in the **absorption profile**. The significant increase in anthelmintic efficacy of MBZ against already encysted *T. spiralis* parasites would be primarily attributed to the improved absorption provided by these innovative formulations, which overcome the limitations of the drug's poor solubility and low bioavailability, resulting in higher plasma concentrations of the active drug, even at low doses. These findings suggest that **the novel MBZ formulations** are suitable for treating ***T. spiralis* infection,** highlighting a potential improvement in the **pharmacological treatment** of **trichinellosis**.

Author Contributions: Methodology, investigation, data curation, conceptualization, AVC, and PAI; writing—original draft preparation, AVC, and MCL; writing- review and editing, LIH; supervision, resources, project administration, funding acquisition, conceptualization, LIH and MCL.

Funding: This research was funded by Universidad Nacional de Rosario (Res C.S. N° 125/2021), and Secretaría de Ciencia, Tecnología e Innovación de la Provincia de Santa Fe (Project N° IO - 2017 – 00220).

Data availability: Data will be made available on request.

Acknowledgments: The authors acknowledge members of the HPLC group for advice and technical support.

Declaration of competing interest: the authors declare that they have no known competing financial interests or personal relationships that could have appeared to influence the work reported in this paper.

References

 doi:10.20944/preprints202504.2256.v1

1. Sun, Z.S.; Wan, E.Y.; Agbana, Y.L.; Zhao, H.Q.; Yin, J.X.; Jiang, T.G.; Li, Q.; Fei, S.W.; Wu, L.B.; Li, X.C.; et al. Global One Health Index for Zoonoses: A Performance Assessment in 160 Countries and Territories. *iScience* **2024**, *27*, doi:10.1016/j.isci.2024.109297.
2. Burgos, L.M.; Farina, J.; Liendro, M.C.; Saldarriaga, C.; Liprandi, A.S.; Wyss, F.; Mendoza, I.; Baranchuk, A. Neglected Tropical Diseases and Other Infectious Diseases Affecting the Heart. The NET-Heart Project: Rationale and Design. *Glob Heart* **2020**, *15*, doi:10.5334/GH.867.
3. Bilska-Zając, E.; Thompson, P.; Rosenthal, B.; Różycki, M.; Cencek, T. Infection, Genetics, and Evolution of Trichinella: Historical Insights and Applications to Molecular Epidemiology. *Infection, Genetics and Evolution* **2021**, *95*, 105080, doi:10.1016/J.MEEGID.2021.105080.
4. Mandal, L.; Biswas, N. Host Immune Responses against Parasitic Infection. *Viral, Parasitic, Bacterial, and Fungal Infections: Antimicrobial, Host Defense, and Therapeutic Strategies* **2023**, 329–339, doi:10.1016/B978-0-323-85730-7.00060-6.
5. Rostami, A.; Gamble, H.R.; Dupouy-Camet, J.; Khazan, H.; Bruschi, F. Meat Sources of Infection for Outbreaks of Human Trichinellosis. *Food Microbiol* **2017**, *64*, 65–71, doi:10.1016/J.FM.2016.12.012.
6. Bruschi, F.; Murrell, K.D. Trichinellosis. *Hunter's Tropical Medicine and Emerging Infectious Diseases* **2020**, 882–884, doi:10.1016/B978-0-323-55512-8.00119-8.
7. Calcagno, M.A.; Bourlot, I.; Taus, R.; Saracino, M.P.; Venturiello, S.M. Description of an Outbreak of Human Trichinellosis in an Area of Argentina Historically Regarded as Trichinella-Free: The Importance of Surveillance Studies. *Vet Parasitol* **2014**, *200*, 251–256, doi:10.1016/J.VETPAR.2013.12.028.
8. Luis Muñoz-Carrillo, J.; Maldonado-Tapia, C.; López- Luna, A.; Jesús Muñoz-Escobedo, J.; Armando Flores-De La Torre, J.; Moreno-García, A. Current Aspects in Trichinellosis. *Parasites and Parasitic Diseases* **2019**, doi:10.5772/INTECHOPEN.80372.
9. Robertson, L.J. Parasites in Food: From a Neglected Position to an Emerging Issue. *Adv Food Nutr Res* **2018**, *86*, 71–113, doi:10.1016/BS.AFNR.2018.04.003.
10. Cretu, C.M. Treatment. *Trichinella and Trichinellosis* **2021**, 417–429, doi:10.1016/B978-0-12-821209-7.00017-2.
11. García, A.; Priotti, J.; Codina, A.V.; Vasconi, M.D.; Quiroga, A.D.; Hinrichsen, L.I.; Leonardi, D.; Lamas, M.C. Synthesis and Characterization of a New Cyclodextrin Derivative with Improved Properties to Design Oral Dosage Forms. *Drug Deliv Transl Res* **2019**, *9*, 273–283, doi:10.1007/S13346-018-0591-8.
12. Priotti, J.; Codina, A. V.; Leonardi, D.; Vasconi, M.D.; Hinrichsen, L.I.; Lamas, M.C. Albendazole Microcrystal Formulations Based on Chitosan and Cellulose Derivatives: Physicochemical Characterization and In Vitro Parasiticidal Activity in Trichinella Spiralis Adult Worms. *AAPS PharmSciTech* **2017**, *18*, 947–956, doi:10.1208/S12249-016-0659-Z.
13. Yousef, F.O.; Ghanem, R.; Al-Sou'od, K.A.; Alsarhan, A.; Abuflaha, R.K.; Bodoor, K.; Assaf, K.I.; El-Barghouthi, M.I. Investigation of Spectroscopic Properties and Molecular Dynamics Simulations of the Interaction of Mebendazole with β-Cyclodextrin. *Journal of the Iranian Chemical Society* **2021**, *18*, 75–86, doi:10.1007/S13738-020-02006-W/METRICS.
14. McRae, K.M.; Good, B.; Hanrahan, J.P.; McCabe, M.S.; Cormican, P.; Sweeney, T.; O'Connell, M.J.; Keane, O.M. Transcriptional Profiling of the Ovine Abomasal Lymph Node Reveals a Role for Timing of the Immune Response in Gastrointestinal Nematode Resistance. *Vet Parasitol* **2016**, *224*, 96–108, doi:10.1016/J.VETPAR.2016.05.014.
15. McRae, K.M.; Good, B.; Hanrahan, J.P.; Glynn, A.; O'Connell, M.J.; Keane, O.M. Response to Teladorsagia Circumcincta Infection in Scottish Blackface Lambs with Divergent Phenotypes for Nematode Resistance. *Vet Parasitol* **2014**, *206*, 200–207, doi:10.1016/J.VETPAR.2014.10.023.
16. McRae, K.M.; McEwan, J.C.; Dodds, K.G.; Gemmell, N.J. Signatures of Selection in Sheep Bred for Resistance or Susceptibility to Gastrointestinal Nematodes. *BMC Genomics* **2014**, *15*, 1–13, doi:10.1186/1471-2164-15-637/TABLES/3.
17. Machado-Silva, J.R.; Neves, R.H.; Da Silva, L.O.; De Oliveira, R.M.F.; Da Silva, A.C. Do Mice Genetically Selected for Resistance to Oral Tolerance Provide Selective Advantage for Schistosoma Mansoni Infection? *Exp Parasitol* **2005**, *111*, 1–7, doi:10.1016/J.EXPPARA.2005.04.003.
18. Gurwitz, D.; McLeod, H.L. Genome-Wide Studies in Pharmacogenomics: Harnessing the Power of Extreme Phenotypes. *Pharmacogenomics* **2013**, *14*, 337–339, doi:10.2217/PGS.13.35.

 doi:10.20944/preprints202504.2256.v1

19. Buchter, V.; Priotti, J.; Leonardi, D.; Lamas, M.C.; Keiser, J. Preparation, Physicochemical Characterization and In Vitro and In Vivo Activity Against Heligmosomoides Polygyrus of Novel Oral Formulations of Albendazole and Mebendazole. *J Pharm Sci* **2020**, *109*, 1819–1826, doi:10.1016/J.XPHS.2020.02.002.
20. García, A.; Leonardi, D.; Salazar, M.O.; Lamas, M.C. Modified β-Cyclodextrin Inclusion Complex to Improve the Physicochemical Properties of Albendazole. Complete in Vitro Evaluation and Characterization. *PLoS One* **2014**, *9*, doi:10.1371/JOURNAL.PONE.0088234.
21. Kang, B.S.; Lee, S.E.; Ng, C.L.; Kim, J.K.; Park, J.S. Exploring the Preparation of Albendazole-Loaded Chitosan-Tripolyphosphate Nanoparticles. *Materials 2015, Vol. 8, Pages 486-498* **2015**, *8*, 486–498, doi:10.3390/MA8020486.
22. US Pharmacopeia (USP) Available online: https://www.usp.org/ (accessed on 12 January 2025).
23. Di Masso, R. Empleo de Un Modelo Murino Original de Argentina En La Caracterización de Fenotipos Complejos. *Journal of Basic and Applied Genetics* **2010**.
24. Vasconi, M.D.; Bertorini, G.; Codina, A. V.; Indelman, P.; Masso, R.J. Di; Hinrichsen, L.I. Phenotypic Characterization of the Response to Infection with Trichinella Spiralis in Genetically Defined Mouse Lines of the CBi-IGE Stock. *Open J Vet Med* **2015**, *05*, 111–122, doi:10.4236/OJVM.2015.55015.
25. Codina, A. V.; Priotti, J.; Leonardi, D.; Vasconi, M.D.; Lamas, M.C.; Hinrichsen, L.I. Effect of Sex and Genotype of the Host on the Anthelmintic Efficacy of Albendazole Microcrystals, in the CBi-IGE Trichinella Infection Murine Model. *Parasitology* **2021**, *148*, 1545–1553, doi:10.1017/S0031182021001128.
26. Codina, A. V.; García, A.; Leonardi, D.; Vasconi, M.D.; Di Masso, R.J.; Lamas, M.C.; Hinrichsen, L.I. Efficacy of Albendazole:β-Cyclodextrin Citrate in the Parenteral Stage of Trichinella Spiralis Infection. *Int J Biol Macromol* **2015**, *77*, 203–206, doi:10.1016/J.IJBIOMAC.2015.02.049.
27. De Ruyck, H.; Daeseleire, E.; De Ridder, H.; Van Renterghem, R. Liquid Chromatographic-Electrospray Tandem Mass Spectrometric Method for the Determination of Mebendazole and Its Hydrolysed and Reduced Metabolites in Sheep Muscle. *Anal Chim Acta* **2003**, *483*, 111–123, doi:10.1016/S0003-2670(02)01018-8.
28. Nguyen, T.N.; Tran, P.; Choi, Y.E.; Park, J.S. Solid Dispersion of Mebendazole via Surfactant Carrier to Improve Oral Bioavailability and in Vitro Anticancer Efficacy. *J Pharm Investig* **2023**, *53*, 443–455, doi:10.1007/S40005-023-00616-Z/METRICS.
29. García, A.; Leonardi, D.; Vasconi, M.D.; Hinrichsen, L.I.; Lamas, M.C. Characterization of Albendazole-Randomly Methylated-β-Cyclodextrin Inclusion Complex and in Vivo Evaluation of Its Antihelmitic Activity in a Murine Model of Trichinellosis. *PLoS One* **2014**, *9*, doi:10.1371/JOURNAL.PONE.0113296.
30. Randazzo, V.R.; Costamagna, S.R. [Methylene Blue Test for the Determination of Viability of Free Larvae of Trichinella Spiralis]. *Rev Argent Microbiol* **2010**, *42*, 95–97, doi:10.1590/S0325-75412010000200005.
31. Sheskin, D.J. (2011) Handbook of Parametric and Non-Parametric Statistical Procedures. 5th Edition, Chapman & Hall/CRC, London. - Search Results - PubMed Available online: https://pubmed.ncbi.nlm.nih.gov/?term=Sheskin%2C+D.J.+%282011%29+Handbook+of+Parametric+and+Non-Parametric+Statistical+Procedures.+5th+Edition%2C+Chapman+%26+Hall%2FCRC%2C+London. (accessed on 13 March 2025).
32. Li, J.; Wang, Z.; Zhang, H.; Gao, J.; Zheng, A. Progress in the Development of Stabilization Strategies for Nanocrystal Preparations. *Drug Deliv* **2021**, *28*, 19–36, doi:10.1080/10717544.2020.1856224.
33. Nyamba, I.; Sombié, C.B.; Yabré, M.; Zimé-Diawara, H.; Yaméogo, J.; Ouédraogo, S.; Lechanteur, A.; Semdé, R.; Evrard, B. Pharmaceutical Approaches for Enhancing Solubility and Oral Bioavailability of Poorly Soluble Drugs. *European Journal of Pharmaceutics and Biopharmaceutics* **2024**, *204*, doi:10.1016/j.ejpb.2024.114513.
34. Gupta, S.; Omar, T.; Zhou, Q.; Scicolone, J.; Callegari, G.; Dubey, A.; Muzzio, F. High-Dose Modified-Release Formulation of a Poorly Soluble Drug via Twin-Screw Melt Coating and Granulation. *Int J Pharm* **2025**, *670*, doi:10.1016/j.ijpharm.2024.125090.
35. Yi, S.; Guo, T.; Wang, Y.; Yang, X.; Liao, Y.; Tang, X.; Zhang, X. A Micrometer Sized Porous β-Cyclodextrin Polymer for Improving Bioavailability of Poorly Soluble Drug. *Carbohydr Polym* **2025**, *350*, doi:10.1016/j.carbpol.2024.123042.
36. Brough, C.; Williams, R.O. Amorphous Solid Dispersions and Nano-Crystal Technologies for Poorly Water-Soluble Drug Delivery. *Int J Pharm* **2013**, *453*, 157–166, doi:10.1016/J.IJPHARM.2013.05.061.

 doi:10.20944/preprints202504.2256.v1

37. Mochizuki, T.; Kusuhara, H. Progress in the Quantitative Assessment of Transporter-Mediated Drug-Drug Interactions Using Endogenous Substrates in Clinical Studies. *Drug Metab Dispos* **2023**, *51*, 1105–1113, doi:10.1124/DMD.123.001285.
38. Lin, J. Pharmacokinetic and Pharmacodynamic Variability: A Daunting Challenge in Drug Therapy. *Curr Drug Metab* **2007**, *8*, 109–136, doi:10.2174/138920007779816002.
39. Gao, Y.; Sun, L.; Qiao, C.; Liu, Y.; Wang, Y.; Feng, R.; Zhang, H.; Zhang, Y. Cyclodextrin-Based Delivery Systems for Chemical and Genetic Drugs: Current Status and Future. *Carbohydr Polym* **2025**, *352*, doi:10.1016/J.CARBPOL.2024.123174.
40. García, A.; Leonardi, D.; Vasconi, M.D.; Hinrichsen, L.I.; Lamas, M.C. Characterization of Albendazole-Randomly Methylated-β-Cyclodextrin Inclusion Complex and in Vivo Evaluation of Its Antihelmitic Activity in a Murine Model of Trichinellosis. *PLoS One* **2014**, *9*, doi:10.1371/JOURNAL.PONE.0113296.
41. Delahousse, J.; Wagner, A.D.; Borchmann, S.; Adjei, A.A.; Haanen, J.; Burgers, F.; Letsch, A.; Quaas, A.; Oertelt-Prigione, S.; Oezdemir, B.C.; et al. Sex Differences in the Pharmacokinetics of Anticancer Drugs: A Systematic Review. *ESMO Open* **2024**, *9*, doi:10.1016/J.ESMOOP.2024.104002.
42. Mauvais-Jarvis, F.; Berthold, H.K.; Campesi, I.; Carrero, J.J.; Dakal, S.; Franconi, F.; Gouni-Berthold, I.; Heiman, M.L.; Kautzky-Willer, A.; Klein, S.L.; et al. Sex- and Gender-Based Pharmacological Response to Drugs. *Pharmacol Rev* **2021**, *73*, 730–762, doi:10.1124/PHARMREV.120.000206.
43. Soldin, O.P.; Chung, S.H.; Mattison, D.R. Sex Differences in Drug Disposition. *J Biomed Biotechnol* **2011**, *2011*, doi:10.1155/2011/187103.
44. Cisneros, E.P.; Morse, B.A.; Savk, A.; Malik, K.; Peppas, N.A.; Lanier, O.L. The Role of Patient-Specific Variables in Protein Corona Formation and Therapeutic Efficacy in Nanomedicine. *J Nanobiotechnology* **2024**, *22*, doi:10.1186/S12951-024-02954-Y.
45. Sharifi, S.; Caracciolo, G.; Pozzi, D.; Digiacomo, L.; Swann, J.; Daldrup-Link, H.E.; Mahmoudi, M. The Role of Sex as a Biological Variable in the Efficacy and Toxicity of Therapeutic Nanomedicine. *Adv Drug Deliv Rev* **2021**, *174*, 337–347, doi:10.1016/J.ADDR.2021.04.028.
46. Liu, J.; Lu, Y.F.; Corton, J.C.; Klaassen, C.D. Expression of Cytochrome P450 Isozyme Transcripts and Activities in Human Livers. *Xenobiotica* **2021**, *51*, 279–286, doi:10.1080/00498254.2020.1867929.
47. Gerges, S.H.; El-Kadi, A.O.S. Sexual Dimorphism in the Expression of Cytochrome P450 Enzymes in Rat Heart, Liver, Kidney, Lung, Brain, and Small Intestine. *Drug Metab Dispos* **2023**, *51*, 81–94, doi:10.1124/DMD.122.000915.
48. Kato, R.; Kamataki, T. Cytochrome P-450 as a Determinant of Sex Difference of Drug Metabolism in the Rat. *Xenobiotica* **1982**, *12*, 787–800, doi:10.3109/00498258209038950.
49. Schwartz, J.B. The Influence of Sex on Pharmacokinetics. *Clin Pharmacokinet* **2003**, *42*, 107–121, doi:10.2165/00003088-200342020-00001.
50. Rose, T.M.; Baranek, M.; Kaka, M.; Shwani, S. Natural Drugs: Trends, Properties, and Decline in FDA Approvals. *J Pharm Sci* **2024**, doi:10.1016/J.XPHS.2024.12.007.
51. Woolsey, S.J.; Mansell, S.E.; Kim, R.B.; Tirona, R.G.; Beaton, M.D. CYP3A Activity and Expression in Nonalcoholic Fatty Liver Disease. *Drug Metabolism and Disposition* **2015**, *43*, 1484–1490, doi:10.1124/DMD.115.065979.
52. Fredericks, J.; Hill, D.E.; Zarlenga, D.S.; Fournet, V.M.; Hawkins-Cooper, D.S.; Urban, J.F.; Kramer, M. *Inactivation of Encysted Muscle Larvae of Trichinella Spiralis in Pigs Using Mebendazole. *Vet Parasitol* **2024**, *327*, doi:10.1016/J.VETPAR.2024.110140.
53. Hess, J.A.; Chandrasekar, P.H.; Mortiere, M.; Molinari, J.A. Comparative Efficacy of Ketoconazole and Mebendazole in Experimental Trichinosis. *Antimicrob Agents Chemother* **1986**, *30*, 953–954, doi:10.1128/AAC.30.6.953.
54. Mccracken, R.O.; Taylor, D.D. Mebendazole Therapy of Parenteral Trichinellosis. *Science* **1980**, *207*, 1220–1222, doi:10.1126/SCIENCE.7355285.
55. Wesołowska, A. Sex-the Most Underappreciated Variable in Research: Insights from Helminth-Infected Hosts. *Vet Res* **2022**, *53*, 94, doi:10.1186/S13567-022-01103-3.

 doi:10.20944/preprints202504.2256.v1

56. Fredericks, J.; Hill, D.E.; Zarlenga, D.S.; Fournet, V.M.; Hawkins-Cooper, D.S.; Urban, J.F.; Kramer, M. *Inactivation of Encysted Muscle Larvae of Trichinella Spiralis in Pigs Using Mebendazole. *Vet Parasitol* **2024**, *327*, doi:10.1016/J.VETPAR.2024.110140.
57. Abou Rayia, D.M.; Saad, A.E.; Ashour, D.S.; Oreiby, R.M. Implication of Artemisinin Nematocidal Activity on Experimental Trichinellosis: In Vitro and in Vivo Studies. *Parasitol Int* **2017**, *66*, 56–63, doi:10.1016/J.PARINT.2016.11.012.
58. de la Torre-Iglesias, P.M.; García-Rodriguez, J.J.; Torrado, G.; Torrado, S.; Torrado-Santiago, S.; Bolás-Fernández, F. Enhanced Bioavailability and Anthelmintic Efficacy of Mebendazole in Redispersible Microparticles with Low-Substituted Hydroxypropylcellulose. *Drug Des Devel Ther* **2014**, *8*, 1467–1479, doi:10.2147/DDDT.S65561.
59. Maki, J.; Yanagisawa, T. Comparative Efficacy of Flubendazole and Mebendazole on Encysted Larvae of Trichinella Spiralis (USA Strain) in the Diaphragm of Mice and Rats. *J Helminthol* **1988**, *62*, 35–39, doi:10.1017/S0022149X00011172.
60. Fornelio, A.C.; Caabeiro, F.R.; Gonzalez, A.J. The Mode of Action of Some Benzimidazole Drugs on Trichinella Spiralis. *Parasitology* **1987**, *95 (Pt 1)*, 61–70, doi:10.1017/S0031182000057541.
61. Beiting, D.P.; Bliss, S.K.; Schlafer, D.H.; Roberts, V.L.; Appleton, J.A. Interleukin-10 Limits Local and Body Cavity Inflammation during Infection with Muscle-Stage Trichinella Spiralis. *Infect Immun* **2004**, *72*, 3129–3137, doi:10.1128/IAI.72.6.3129-3137.2004.
62. Pozio, E.; Sacchini, D.; Sacchi, L.; Tamburrini, A.; Alberici, F. Failure of Mebendazole in the Treatment of Humans with Trichinella Spiralis Infection at the Stage of Encapsulating Larvae. *Clin Infect Dis* **2001**, *32*, 638–642, doi:10.1086/318707.
63. Bruschi, F. Trichinella and Trichinellosis. **2021**.
64. Martinez-Fernandez, A.R.; Samartin-Duran, M.L.; Toro Rojas, M.; Ubeira, F.M.; Rodriguez Cabeiro, F. Histopathological Modifications Induced Ny Mebendazole and Niridazole on Encysted Larvae of Trichinella Spiralis in CD-1 Mice. *Wiad Parazytol* **1987**, *33*.